Haploinsufficiency of the NOTCH1 receptor as a cause of Adams-Oliver syndrome with variable cardiac anomalies

Southgate *et al.* *NOTCH1* mutations in Adams-Oliver syndrome

Laura Southgate, PhD[1,2]; Maja Sukalo, Dipl-Biol[3]; Anastasios S. V. Karountzos, MSc[4]; Edward J. Taylor, PhD[4]; Claire S. Collinson, MSc[1]; Deborah Ruddy, MRCP, PhD[5]; Katie M. Snape, MRCP, PhD[6]; Bruno Dallapiccola, MD[7]; John L. Tolmie, FRCP[8,17]; Shelagh Joss, MRCP[8]; Francesco Brancati, MD, PhD[9]; M. Cristina Digilio, MD[10]; Luitgard M. Graul-Neumann, MD[11]; Leonardo Salviati, MD, PhD[12]; Wiltrud Coerdt, MD, PhD[13]; Emmanuel Jacquemin, MD, PhD[14,15]; Wim Wuyts, PhD[16]; Martin Zenker, MD[3]; Rajiv D. Machado, PhD[4,*]; Richard C. Trembath, FRCP, FMedSci[2,5,*]

AUTHOR AFFILIATIONS:

[1]Division of Genetics and Molecular Medicine, King's College London, Faculty of Life Sciences and Medicine, Guy's Hospital, London, UK

[2]Barts and The London School of Medicine and Dentistry, Queen Mary University of London, Charterhouse Square, London, UK

[3]Institute of Human Genetics, Otto-von-Guericke-Universität Magdeburg, University Hospital Magdeburg, Magdeburg, Germany

[4]School of Life Sciences, University of Lincoln, Brayford Pool, Lincoln, UK

[5]Department of Clinical Genetics, Guy’s Hospital, Guy’s and St Thomas’ NHS Foundation Trust, London, UK

[6]Department of Clinical Genetics, South West Thames Regional Genetics Service, St George’s Healthcare NHS Trust, London, UK

[7]Scientific Directorate, Bambino Gesù Children’s Hospital, IRCCS, Rome, Italy

[8]South West of Scotland Clinical Genetics Service, Southern General Hospital, Glasgow, UK

[9]Department of Medical, Oral and Biotechnological Sciences, Gabriele d'Annunzio University of Chieti-Pescara, Chieti, Italy

[10]Medical Genetics, Bambino Gesù Children's Hospital, IRCCS, Rome, Italy

[11]Ambulantes Gesundheitszentrum der Charité-Universitätsmedizin Berlin, Berlin, Germany

[12]Clinical Genetics Unit, Department of Woman and Child Health, University of Padova, Padova, Italy

[13]Institute of Human Genetics, Mainz University Medical Center, Mainz, Germany

[14]Pediatric Hepatology and Liver Transplantation Unit, Bicêtre Hospital, Assistance Publique - Hôpitaux de Paris, Hepatinov, Le Kremlin Bicêtre, France

[15]Inserm U1174, University Paris-Sud 11, Orsay, France

[16]Department of Medical Genetics, University and University Hospital of Antwerp, Edegem, Belgium

[17]Tragically died during the preparation of this manuscript

[*]Drs Machado and Trembath contributed equally as senior authors

CORRESPONDING AUTHOR:

Prof. Richard C. Trembath

Barts and The London School of Medicine and Dentistry, Queen Mary University of London, Old Anatomy Building, Charterhouse Square, London. EC1M 6BQ, United Kingdom

Tel: +44 2078822258; Fax: +44 2078827187; Email: vp-health@qmul.ac.uk

WORD COUNT: 6,980 words

JOURNAL SUBJECT CODES: [6] Cardiac development; [109] Clinical genetics

ABSTRACT:

Background: Adams-Oliver syndrome (AOS) is a rare disorder characterized by congenital limb defects and scalp cutis aplasia. In a proportion of cases, notable cardiac involvement is also apparent. Despite recent advances in the understanding of the genetic basis of AOS, for the majority of affected subjects the underlying molecular defect remains unresolved. This study aimed to identify novel genetic determinants of AOS.

Methods and Results: Whole-exome sequencing was performed for 12 probands, each with a clinical diagnosis of AOS. Analyses led to the identification of novel heterozygous truncating *NOTCH1* mutations (c.1649dupA and c.6049_6050delTC) in two kindreds in which AOS was segregating as an autosomal dominant trait. Screening a cohort of 52 unrelated AOS subjects, we detected 8 additional unique *NOTCH1* mutations, including three *de novo* amino-acid substitutions, all within the ligand-binding domain. Congenital heart anomalies were noted in 47% (8/17) of *NOTCH1*-positive probands and affected family members. In leucocyte-derived RNA from subjects harboring *NOTCH1* extracellular domain mutations, we observed significant reduction of *NOTCH1* expression, suggesting instability and degradation of mutant mRNA transcripts by the cellular machinery. Transient transfection of mutagenized *NOTCH1* missense constructs also revealed significant reduction in gene expression. Mutant *NOTCH1* expression was associated with down-regulation of the Notch target genes *HEY1* and *HES1*, indicating that *NOTCH1*-related AOS arises through dysregulation of the Notch signaling pathway.

Conclusions: These findings highlight a key role for *NOTCH1* across a range of developmental anomalies that include cardiac defects, and implicate NOTCH1 haploinsufficiency as a likely molecular mechanism for this group of disorders.

KEY WORDS: Congenital heart defects; Human genetics; Adams-Oliver syndrome; Haploinsufficiency; NOTCH1

INTRODUCTION:

Adams-Oliver syndrome (AOS; MIM 100300) is a rare developmental disorder, characterized by a range of abnormalities that include cranial aplasia cutis congenita (ACC) and terminal transverse limb defects (TTLD).[1,2] The spectrum of defects observed implies dysregulation of multiple developmental pathways. Congenital heart defects (CHDs) have been reported in conjunction with AOS in up to 20% of cases and, when present, represent a serious mortality risk.[3,4] Cardiac defects are also commonly associated with systemic structural vascular abnormalities, of which cutis marmorata telangiectatica congenita (CMTC) is the most frequently described.[5] AOS primarily segregates as an autosomal dominant trait with variable phenotypic expression. A small number of kindreds are consistent with autosomal recessive disease gene transmission. In addition, sporadic cases with comparable clinical features indicate the occurrence of *de novo* mutations in causative disease genes.

The molecular genetic basis of AOS appears heterogeneous and, to date, defects within five genes have been reported, providing limited insight as to the molecular mechanisms underlying these important aspects of early development. Mutations of the *ARHGAP31* and *DOCK6* genes underlie a proportion of AOS cases displaying autosomal dominant and recessive inheritance, respectively.[6,7] Both ARHGAP31 and DOCK6 regulate the activity of the Rho GTPases Cdc42 and Rac1, which cycle between active, GTP-bound and inactive, GDP-bound states through the opposing modes of action of guanine nucleotide exchange factors (GEFs) and GTPase-activating proteins (GAPs). We have previously demonstrated that ARHGAP31 mutations cause AOS through a gain-of-function mechanism, which leads to an accumulation of inactive GTPase, disrupting actin cytoskeletal dynamics.[6] Mutations in DOCK6 result in a more severe, multi-systemic phenotype due to a homozygous loss of GEF function.[7]

More recently, the Notch signaling pathway has been implicated in AOS pathogenesis by the discovery of heterozygous alterations in the *RBPJ* gene, encoding the major transcription factor for Notch.[8] Missense mutations within the DNA-binding domain of RBPJ result in impaired binding ability of the transcription factor to the *HES1* promoter, likely disrupting the regulation of Notch target genes downstream.[8] Moreover, two independent studies have identified homozygous mutations

of *EOGT*, encoding an EGF domain-specific enzyme demonstrated as critical in the glycosylation of Notch1 in mammalian cells.[9,10] Most recently, a report by Stittrich *et al.* identified mutations of the *NOTCH1* gene in a proportion of an AOS cohort.[11]

These studies have provided some important insights into the molecular processes key to the development of AOS. However, despite congenital heart anomalies affecting approximately 1 in 5 subjects with AOS, the *ARHGAP31*- and *RBPJ*-positive pedigrees reported in the literature have a notable lack of cardiovascular involvement.[6,8,12] Although the majority of these mutation carriers may not have been assessed by cardiac imaging, these data implicate distinct regulatory systems in the pathogenesis of autosomal dominant AOS with congenital heart defects. We designed an exome-wide based study, to further define the genetic mechanisms relevant to the pathogenesis of AOS. Through this work, we identified novel heterozygous mutations of *NOTCH1*, providing independent verification of a critical role for this gene as a common cause of AOS in both autosomal dominant and sporadic cases. We have further used gene expression studies to examine the impact of *NOTCH1* mutation on downstream signaling and demonstrated a pathogenic effect in RNA extracted from AOS subjects harboring *NOTCH1* defects. These cases display a striking genotype-phenotype correlation with a high prevalence of cardiac and vascular anomalies, highlighting the importance of Notch signaling in cardiovascular development and demonstrating a novel role for *NOTCH1* in multiple developmental processes that include scalp and limb formation.

METHODS:

Patient cohorts

Exome sequencing was performed for 12 unrelated probands, diagnosed with autosomal dominant AOS and negative for *ARHGAP31* and *RBPJ* mutations. Criteria for diagnosis were according to the guidelines by Snape *et al*.[5] Subsequent mutation screening of the *NOTCH1* coding regions comprised a cohort of 52 additional individuals with a diagnosis of AOS (n=11 autosomal dominant, n=41 isolated cases with no known family history). Cardiac clinical evaluation and echocardiography of

NOTCH1-positive patients and family members was conducted at specialist cardiology centers (UK, Germany, Italy, France) following referral by the respective consultant clinical geneticist. The study complies with the Declaration of Helsinki and informed written consent was obtained from all participants before taking part. The research protocol was approved by the local ethics committees (NRES Committee London (Bromley), UK and the Ethics Board of the Medical Faculty of the University of Erlangen, Germany). Patient samples were collected as either saliva (Oragene DNA collection kit, DNA Genotek) or blood, and genomic DNA was extracted according to standard protocols.

Exome sequencing and mutation detection

Exome libraries were generated with the SureSelect Human All Exon Target Enrichment kit (Agilent Technologies) using genomic DNA extracted from peripheral blood. Paired-end sequence reads were generated on an Illumina HiSeq 2000. Read alignment to the reference genome (hg19) and variant calling were performed as described previously,[6] with variant annotation completed using the ANNOVAR software.[13] Sequence variants were compared against publicly available databases (HapMap, 1000 Genomes Project, dbSNP, the NHLBI Exome Sequencing Project (ESP) Exome Variant Server, and an in-house repository of 400 exomes) to assess their novelty. Candidate genes were prioritized on the basis of novel truncating mutations (frameshift, nonsense, splice-site) in two or more independent probands. Of these, *NOTCH1* was taken forward for further study due to compelling biological relevance to AOS pathogenesis. Validation of variant segregation and mutation screening of all *NOTCH1* coding regions and intron-exon boundaries was performed by direct DNA sequencing using BigDye Terminator v3.1 chemistry on an ABI3730xl (Applied Biosystems).

Mutagenesis and cell culture

Wild-type *NOTCH1* cDNA in pFN1A (Kazusa DNA Research Institute)[14] was purchased from Promega. Identified AOS missense variants were introduced by site-directed mutagenesis using the QuikChange II XL kit (Agilent Technologies). Primer details are available on request. Cells were

maintained at 37°C in a humidified incubator with 5% CO_2. Human endometrioid cancer (HeLa) cells were cultured in Dulbecco's modified Eagle's medium (DMEM) with Glutamax (Gibco Life Technologies), supplemented with 10% fetal bovine serum. HeLa cells were seeded in 100 mm dishes and grown to 80% confluence. Transient transfection was performed using FuGene HD transfection reagent (Promega) and transfected cells were incubated for 48 hours before harvesting for RNA extraction.

Gene-expression analysis

Total RNA was extracted from 2.5 ml of peripheral blood from *NOTCH1*-positive patients and a 26 year old clinically unaffected female control using the PAXgene Blood RNA System (PreAnalytiX), following the manufacturer's guidelines. For mutagenized constructs, RNA was extracted from transfected cells with the RNeasy Mini kit (Qiagen), according to the manufacturer's instructions. 500 ng of RNA was used for first strand cDNA synthesis with the High Capacity cDNA Reverse Transcription kit (Applied Biosystems). Quantitative real-time PCR was performed on a StepOnePlus real-time PCR machine (Applied Biosystems) using double-dye Taqman-style detection chemistry with the PrimerDesign 2x Precision Mastermix and custom-designed probe sets for *NOTCH1*, *HEY1* and *HES1* mRNAs (PrimerDesign). *GAPDH* and *ACTB* house-keeping genes were used for normalization in mRNA relative quantifications using SDS v2.2 software. Gene of interest expression levels for patient and mutagenized samples were calculated by the $2^{-\Delta\Delta Ct}$ method relative to the wild-type baseline. Statistical analysis of real-time data was performed using a Mann-Whitney test to generate two-tailed *p* values (VassarStats software).

RESULTS:

Clinical features of *NOTCH1* positive families

The proband of family 1 (1-II:1) displayed cutis aplasia and marked TTLD at birth. The sibling 1-II:2 was also born with a severe cutaneous and bony scalp defect, with TTLD affecting both feet. On

examination, the obligate carrier mother (1-I:3) exhibited no scalp or limb defects, but was found to have an unexplained heart murmur. Subject 1-I:1 had died at 5 months due to a congenital heart defect, but no further details were available. Patient 1-II:4 presented with syndactyly of the left hand and both feet, and CMTC on the abdomen and legs. Echocardiography revealed mild aortic stenosis and mild aortic regurgitation. Similar digit abnormalities and scalp ACC were displayed by subject 1-III:1. Although 1-III:2 appeared clinically normal on examination, sonography of the heart also revealed mild aortic regurgitation (Table 1).

Family 2 has been previously described by Dallapiccola *et al*.[15] The proband (2-II:1) and his mother both exhibited ACC of the midline region of the scalp and cardiac investigation by ultrasonography identified coarctation of the aorta in both individuals. The mother (2-I:2) also had a vascular anomaly consisting of duplication of the right femoral artery. Surgical intervention to repair the aortic coarctation and femoral artery duplication were conducted at 14 and 17 years of age, respectively. The cardiac defect in subject 2-II:1 resembled the so-called 'Shone's complex', an anatomic variant consisting of multiple levels of left-sided obstructive CHDs,[3,18] including aortic coarctation, bicuspid aortic valve, and parachute non-stenotic mitral valve with mild regurgitation. Coarctectomy was performed at 5 months of age.

Patient 3-III:1 was born with a large area of scalp ACC with an underlying calvarial defect and shortened distal phalanges of the toes (Figure 1). A recent echocardiography detected no obvious abnormality. The obligate carrier father (3-II:2) was clinically normal and cardiology examination was negative for cardiac defects. The relative 3-II:3 was considered to be affected with minor terminal hypoplasia of the phalanges of some toes but no cardiac anomaly was detected on sonography.

The proband of family 4 (4-II:1) presented with scalp ACC of the posterior parietal region and brachydactyly of both hands. Cardiovascular abnormalities included coarctation of the aorta, valvular aortic stenosis, parachute mitral valve with valvular insufficiency, and a subaortic membranous ventricular septal defect (VSD), also indicative of Shone's complex. Aortic coarctation was operated at 15 days of life; aortic valvulotomy and intervention for VSD were performed at 9 years of age. Aortic valve substitution surgery was completed at 23 years old. Echocardiography in the mother (4-

I:2) revealed valvular aortic stenosis with thick fibrotic semilunar valves, moderate aortic valve insufficiency, and mild to moderate left ventricular hypertrophy (Table 1).

Specific clinical features of sporadic cases 5–11 are summarized in Table 1. Representative images of the limb and scalp defects observed across our AOS cohort are shown in Figure 1.

Identification of novel *NOTCH1* variants

The analysis of exome profiles of affected male probands from families 1 and 2 identified novel heterozygous variants (c.1649dupA; p.Y550* and c.6049_6050delTC; p.S2017Tfs*9) in the *NOTCH1* gene (NM_017617.3). Both mutations are predicted to result in premature stop codons of the mRNA transcript. Examination of available members of family 1 confirmed segregation of the c.1649dupA mutation with the phenotype (Figure 2). Unfortunately, DNA was not available from the affected mother of proband 2-II:1 for segregation analysis of the c.6049_6050delTC variant.

Subsequent mutation screening of the *NOTCH1* coding regions was performed in an extended replication cohort of 52 individuals with a clear clinical diagnosis of AOS. Novel *NOTCH1* heterozygous variants were identified in 9 additional subjects. Taken together with the exome data, we report a total of ten distinct heterozygous mutations in the *NOTCH1* gene, one of which (c.1343G>A; p.R448Q) is recurrent, in 4 autosomal dominant families and 7 apparently sporadic cases with no known family history (Figure 2; Table I in the Data Supplement). All variants were confirmed by independent Sanger sequencing and absent from public variant databases. In families, segregation of the observed variant was consistent with the disease phenotype where DNA from multiple family members was available (Figure 2). In AOS mutation carriers with no family history of AOS or isolated cardiovascular disease, the sequencing of available parental DNA demonstrated that three mutations occurred *de novo*, namely c.1343G>A (p.R448Q) in proband 5-II:1, c.1345T>C (p.C449R) in proband 6-II:1 and c.1367G>A (p.C456Y) in proband 10-II:1. In Family 3, two unaffected paternal uncles and two clinically normal siblings of the proband 3-III:1 were negative for the c.4120T>C (p.C1374R) mutation (data not shown). However, the unaffected obligate carrier father (3-II:2) was confirmed to carry the mutation. Similarly, the unaffected mother of subject 7-II:1

was found to harbor the c.1220C>G (p.P407R) variant. Cardiovascular assessment of 3-II:2 and 7-I:2 by echocardiography detected no underlying cardiac abnormality, confirming that these mutation carriers are phenotypically normal and demonstrating incomplete penetrance for mutations in this gene.

NOTCH1 missense mutations are located within critical functional domains

Five of the six missense mutations identified in this study are predicted to be pathogenic by MutationTaster2,[19] PolyPhen-2,[20] and/or SIFT prediction software[21] (Table II in the Data Supplement). The affected amino acids are located across the length of the receptor, in the main situated within the extracellular EGF-repeat domain. Specifically, four mutations (p.P407R, p.R448Q, p.C449R and p.C456Y) occur in or adjacent to the ligand-binding domain, specified by EGF repeats 11-13 (Figure 3A, Figure 4). The majority are strongly conserved across species and lie within highly conserved domains of the protein (Figure 3B). Further, three amino acid substitutions (p.C449R, p.C456Y and p.C1374R) affect cysteine residues, which are likely to disrupt disulfide bonds that are critical for the structure of EGF-like domains (Figure 4). By contrast, the p.A1740S mutation is located within the transmembrane domain and, while conserved across mammalian species, is not conserved in other vertebrate species and has a less clear impact upon the structural integrity of the receptor so remains a variant of unknown significance (Figure 3).

NOTCH1 haploinsufficiency is implicated in AOS pathogenesis

To assess the level of mutant mRNA transcripts, we conducted quantitative real-time PCR studies using RNA extracted from peripheral blood of three patients harboring *NOTCH1* mutation (c.1343G>A and c.1649dupA (*2 cases*)). *NOTCH1* transcript levels were significantly reduced by comparison to an unaffected control individual, demonstrating approximately 50% expression in all samples tested (Figure 5A). Whilst institutional ethical constraints precluded detailed cardiac evaluation of the control subject, it was made clear by personal testimony that there was no family history of developmental abnormalities relating to AOS-CHD. We additionally performed transient

transfection of mutagenized *NOTCH1* constructs to examine the functional impact of missense mutations for which patient RNA was not available. Real-time PCR of RNA extracted from transfected cells also showed a significant decrease of *NOTCH1* expression when compared to cells transfected with a full-length wild-type construct and provided independent verification of *NOTCH1* down-regulation for the c.1343G>A mutation (Figure I in the Data Supplement).

To further interrogate the effect of *NOTCH1* mutations on downstream signaling factors, we next performed gene expression studies to quantify the levels of *HEY1* and *HES1* transcript in patient-derived RNA samples. Subjects harboring the c.1649dupA frameshift mutation exhibited a particularly marked reduction of *HEY1* transcript levels by comparison to wild-type control (p=0.0004). By contrast, down-regulation of *HEY1* expression was less profound for the c.1343G>A missense mutation (Figure 5B). In addition, *HES1* mRNA levels were reduced in the c.1649dupA patients (p=0.0004); however, no significant deviation to the wild-type control was observed in the c.1343G>A sample (Figure 5C).

DISCUSSION:

Molecular genetic studies of AOS have successfully provided vital insights into the pathways relevant to the pathogenesis of this serious disorder of morphogenesis, through the identification of multiple causative genes. Yet, there remains substantial unexplained locus heterogeneity with the underlying molecular genetic determinants still uncharacterized for the majority of cases. This degree of locus heterogeneity is uncommon for a rare disorder and suggests that AOS may represent a cluster of phenotypes with a related etiology, analogous to the RASopathies or ciliopathies.[23,24]

Herein, we report 10 novel germline *NOTCH1* mutations in a patient cohort with autosomal dominant and sporadic forms of AOS. By comparison to AOS cases reported in the literature (13-20%),[3-5,25,26] a significantly higher proportion of probands (5/11; 45%) presented with a congenital heart abnormality (Table 1). Similarly, cardiovascular anomalies were identified in 47% (8/17) of all affected variant carriers, thereby indicating that *NOTCH1* variants may represent a distinct subtype of

AOS associated with cardiac malformations. A number of vascular complications, including CMTC and portal vein abnormalities, were additionally observed in *NOTCH1*-positive cases. Importantly, two of the probands in this study and two related mutation carriers have not undergone echocardiographic assessment; therefore we are unable to define the exact proportion of *NOTCH1*-positive cases with cardiovascular defects. In contrast to other gene reports, these patients predominantly demonstrate ACC with mild TTLD, affecting only terminal phalanges with nail hypoplasia (Figure 1). This study is further corroborated by a recent report of distinct *NOTCH1* mutations in 5 kindreds with AOS and cardiac spectrum defects.[11]

Emerging evidence is accumulating to implicate defects of the Notch signaling pathway in the pathogenesis of AOS. The Notch family of single-pass transmembrane receptors is well documented as playing a vital role in multiple cellular processes during embryogenesis and Notch pathway members have an established role in development of the cardiovascular system.[27] Mutations in a subset of Notch components have been shown to underlie CHDs in both mice and humans but in exclusion of limb and scalp developmental abnormalities. For example, variants in the *JAG1* gene, encoding a Notch ligand, underlie the majority of cases of Alagille syndrome[28] whilst endothelial-specific deletion of *Jag1* in the mouse leads to embryonic lethality and cardiovascular defects.[29] *NOTCH2* mutations account for a proportion of Alagille syndrome cases;[30] however, distinct truncating variants in the terminal exon of *NOTCH2* also lead to the osteolytic developmental disorder Hajdu-Cheney syndrome, indicating pleiotropic effects analogous to the *NOTCH1* receptor.[31,32] Of interest, mice homozygous for a targeted *Jag2* deletion die perinatally due to craniofacial abnormalities and syndactyly of the fore- and hindlimbs, consistent features of the AOS spectrum.[33] Furthermore, both Notch1 and Notch2 play key roles during mouse limb development in the regulation of apoptosis, a process mediated by Notch signaling through Jag2 in the apical ectodermal ridge,[34,35] and the positive regulation of vascular growth through the promotion of angiogenesis and osteogenesis in bone.[36] Despite numerous studies in lower organisms, the function of NOTCH1 during human fetal development remains to be fully elucidated.

In mammalian cells, canonical signaling through the Notch family (Notch1-4) is stimulated by

ligand binding at the cell surface, which leads to proteolytic cleavage of the Notch intracellular domain (NICD), allowing for the formation of a transcriptional complex with RBPJ and co-activators (Figure 6).[37] RBPJ is known to regulate the expression of the basic helix-loop-helix (bHLH) transcription factors *HES1* and *HEY1*, both of which are related to the *Drosophila* hairy and enhancer of split 1 gene. The stimulation of *HES1* and *HEY1* gene expression is therefore a direct readout of Notch signaling activation.

In this study, we report predicted protein truncating mutations (4/10) most likely to be subject to nonsense-mediated decay. The N-terminal ligand-binding domain of NOTCH1 consists of a series of 36 EGF-like repeats. The majority (5/6) of the missense mutations identified in this study affect residues located within EGF domains of the receptor. These individual domains are characterized by a core β-pleated sheet, three disulfide bonds along with a series of variable loops.[38] Within this region, EGF repeats 11-13 have been shown to be implicated with chelating Ca^{2+} which is essential for the maintenance of NOTCH1 function.[38,39] Three of the identified amino acid substitutions resulting in AOS (p.R448Q, p.C449R and p.C456Y) lie within EGF11 and potentially perturb function by disrupting the tertiary structure and affecting Ca^{2+} binding and/or ligand interaction. The X-ray structure of this region of wild-type NOTCH1 indicates that the side chains of Arg448 and Glu424 interact electrostatically (Figure 4),[22] thereby it is anticipated that the p.R448Q mutant is unstable. Similarly, the p.C449R and p.C456Y mutations will likely abolish the disulfide bonds between Cys440 and Cys449, and between Cys456 and Cys467, respectively, thereby disrupting the stability of the adjacent Ca^{2+} coordinated by the side chains Asp469, Glu455 and Asp452 (Figure 4). Whilst the 3-dimensional structure of the EGF35 region has not been experimentally resolved, it is anticipated that a similar effect would be seen with the Cys1374 mutation. Taken together, these observations imply that the majority of missense mutations have a substantial effect on the structural integrity vital to NOTCH1 activity. Determining the functional impact of the transmembrane domain mutation p.A1740S is outside the scope of this study and is therefore of unknown significance.

The 36 EGF-like repeats can be modified by the addition of an O-glucose sugar between the first and second conserved cysteines, and an O-fucose between the second and third cysteines, which

is essential for normal Notch function.[40] Similarly, the target motif $C_5XXGXS/TGXXC_6$, located between the fifth and sixth conserved cysteines has been shown to be recognized by EOGT in both *Drosophila* and mouse.[41] EOGT functions as an O-linked N-acetylglucosamine (GlcNAc) transferase, which catalyses the addition of an O-GlcNAc moiety.[42] Although EOGT has not yet been formally demonstrated to target human Notch, it is notable that 4 of the 5 EGF-domain specific missense mutations identified here are located within this target motif, suggestive of a convergence of pathways previously implicated in the development of AOS (Figure 3B).

To examine the effect of identified mutations on Notch signaling, we have performed gene expression studies and demonstrated that *NOTCH1* expression is down-regulated in AOS subjects harboring *NOTCH1* mutation *in vivo*, by comparison to a single healthy control female, aged 26 years. While it is not uncommon to use a single control in real-time PCR studies, we acknowledge that these findings might have been strengthened by employing additional controls as part of the experimental design. The data generated are corroborated by transient transfection studies of mutant constructs and, together, support the prediction of transcript loss by nonsense-mediated decay or, in the case of missense mutations, potential perturbation of mRNA stability.[43] This observation is underpinned by a reduction of *HEY1* and, to a lesser extent, *HES1* transcript levels. Of interest, perturbation of both *HEY1* and *HES1* expression vary between the mutations tested, indicating allele-specific effects on downstream signaling. These data, whilst preliminary due in part to limited patient sample availability, suggest that down-regulation of *HEY1* is a common mechanism in AOS. *HEY1* is known to have a prominent role in cardiovascular development, with *Hey1*/*Hey2* double-knockout mice exhibiting defects of vasculogenesis and remodeling, particularly in the head region.[44] Moreover, these results are compatible with the hypothesis that dysregulated Notch signaling caused by identified mutations is mediated via the transcription factor RBPJ, a known causal factor in AOS pathogenesis. Taken together, these data offer support for loss-of-function or haploinsufficiency of NOTCH1 as an important factor in AOS pathogenesis, and provide a compelling genotype-phenotype correlation between *NOTCH1* mutation and AOS subjects with cardiac anomalies, which warrants further epidemiological investigation. As the overall study group herein has not been intensively

examined for cardiac complications, these latter conclusions are at present indicative and will benefit from existing and future international collaboration.

This report establishes *NOTCH1* mutation as the primary cause of AOS, accounting for 17% of cases in our cohort, and an important genetic factor in AOS with associated cardiovascular complications. Functional studies have indicated links to related genes associated with this condition, which together emphasize the central importance of the Notch signaling cascade in a series of key developmental systems in human embryogenesis.

ACKNOWLEDGMENTS:

The authors would like to express their thanks to the patients and families for participating in this study and to the various clinicians involved in the European AOS Consortium, for sharing additional patient samples that have not been reported here. The authors acknowledge use of Biomedical Research Centre (BRC) Core Facilities provided by the financial support from the Department of Health via the National Institute for Health Research (NIHR) comprehensive BRC award to Guy's and St Thomas' NHS Foundation Trust in partnership with King's College London and King's College Hospital NHS Foundation Trust.

FUNDING SOURCES:

This work was supported by the British Heart Foundation [RG/08/006/25302 to R.C.T.], the German Research Foundation [DFG; ZE 524/2-3 to M.Z.] and a Wellcome Trust Strategic Award [102627/Z/13/Z to R.C.T.]. A.S.V.K. is the recipient of a PrimerDesign Gold level student sponsorship. E.J.T. is a Royal Society University Research Fellow. R.C.T. held a Senior Investigator Award from the NIHR.

DISCLOSURES:

No conflicts of interest declared.

REFERENCES:

1. Adams FH, Oliver CP. Hereditary deformities in man due to arrested development. *J Hered*. 1945;36:3-7.

2. Martínez-Frías ML, Arroyo Carrera I, Muñoz-Delgado NJ, Nieto Conde C, Rodríguez-Pinilla E, Urioste Azcorra M, et al. [The Adams-Oliver syndrome in Spain: the epidemiological aspects]. *An Esp Pediatr*. 1996;45:57-61.

3. Lin AE, Westgate MN, van der Velde ME, Lacro RV, Holmes LB. Adams-Oliver syndrome associated with cardiovascular malformations. *Clin Dysmorphol*. 1998;7:235-241.

4. Digilio MC, Marino B, Dallapiccola B. Autosomal dominant inheritance of aplasia cutis congenita and congenital heart defect: a possible link to the Adams-Oliver syndrome. *Am J Med Genet A*. 2008;146A:2842-2844.

5. Snape KM, Ruddy D, Zenker M, Wuyts W, Whiteford M, Johnson D, et al. The spectra of clinical phenotypes in aplasia cutis congenita and terminal transverse limb defects. *Am J Med Genet*. 2009;149A:1860-1881.

6. Southgate L, Machado RD, Snape KM, Primeau M, Dafou D, Ruddy DM, et al. Gain-of-function mutations of ARHGAP31, a Cdc42/Rac1 GTPase regulator, cause syndromic cutis aplasia and limb anomalies. *Am J Hum Genet*. 2011;88:574-585.

7. Shaheen R, Faqeih E, Sunker A, Morsy H, Al-Sheddi T, Shamseldin HE, et al. Recessive mutations in DOCK6, encoding the guanidine nucleotide exchange factor DOCK6, lead to abnormal actin cytoskeleton organization and Adams-Oliver syndrome. *Am J Hum Genet*. 2011;89:328-333.

8. Hassed SJ, Wiley GB, Wang S, Lee JY, Li S, Xu W, et al. RBPJ mutations identified in two families affected by Adams-Oliver syndrome. *Am J Hum Genet*. 2012;91:391-395.

9. Shaheen R, Aglan M, Keppler-Noreuil K, Faqeih E, Ansari S, Horton K, et al. Mutations in EOGT confirm the genetic heterogeneity of autosomal-recessive Adams-Oliver syndrome. *Am J Hum Genet*. 2013;92:598-604.

10. Cohen I, Silberstein E, Perez Y, Landau D, Elbedour K, Langer Y, et al. Autosomal recessive Adams-Oliver syndrome caused by homozygous mutation in EOGT, encoding an EGF domain-specific O-GlcNAc transferase. *Eur J Hum Genet*. 2014;22:374-378.

11. Stittrich AB, Lehman A, Bodian DL, Ashworth J, Zong Z, Li H, et al. Mutations in NOTCH1 cause Adams-Oliver syndrome. *Am J Hum Genet*. 2014;95:275-284.

12. Isrie M, Wuyts W, Van Esch H, Devriendt K. Isolated terminal limb reduction defects: extending the clinical spectrum of Adams-Oliver syndrome and ARHGAP31 mutations. *Am J Med Genet A*. 2014;164A:1576-1579.

13. Wang K, Li M, Hakonarson H. ANNOVAR: functional annotation of genetic variants from high-throughput sequencing data. *Nucleic Acids Res*. 2010;38:e164.

14. Nagase T, Yamakawa H, Tadokoro S, Nakajima D, Inoue S, Yamaguchi K, et al. Exploration of human ORFeome: high-throughput preparation of ORF clones and efficient characterization of their protein products. *DNA Res*. 2008;15:137-149.

15. Dallapiccola B, Giannotti A, Marino B, Digilio C, Obregon G. Familial aplasia cutis congenita and coarctation of the aorta. *Am J Med Genet*. 1992;43:762-763.

16. Girard M, Amiel J, Fabre M, Pariente D, Lyonnet S, Jacquemin E. Adams-Oliver syndrome and hepatoportal sclerosis: occasional association or common mechanism? *Am J Med Genet A*. 2005;135:186-189.

17. Franchi-Abella S, Fabre M, Mselati E, De Marsillac ME, Bayari M, Pariente D, et al. Obliterative portal venopathy: a study of 48 children. *J Pediatr*. 2014;165:190-193 e2.

18. Shone JD, Sellers RD, Anderson RC, Adams P, Jr., Lillehei CW, Edwards JE. The developmental complex of "parachute mitral valve," supravalvular ring of left atrium, subaortic stenosis, and coarctation of aorta. *Am J Cardiol*. 1963;11:714-725.

19. Schwarz JM, Cooper DN, Schuelke M, Seelow D. MutationTaster2: mutation prediction for the deep-sequencing age. *Nat Methods*. 2014;11:361-362.

20. Adzhubei IA, Schmidt S, Peshkin L, Ramensky VE, Gerasimova A, Bork P, et al. A method and server for predicting damaging missense mutations. *Nat Methods*. 2010;7:248-249.

21. Kumar P, Henikoff S, Ng PC. Predicting the effects of coding non-synonymous variants on protein function using the SIFT algorithm. *Nat Protoc*. 2009;4:1073-1081.

22. Cordle J, Johnson S, Tay JZ, Roversi P, Wilkin MB, de Madrid BH, et al. A conserved face of the Jagged/Serrate DSL domain is involved in Notch trans-activation and cis-inhibition. *Nat Struct Mol Biol*. 2008;15:849-857.

23. Zenker M. Clinical manifestations of mutations in RAS and related intracellular signal transduction factors. *Curr Opin Pediatr*. 2011;23:443-451.

24. Davis EE, Katsanis N. The ciliopathies: a transitional model into systems biology of human genetic disease. *Curr Opin Genet Dev*. 2012;22:290-303.

25. Patel MS, Taylor GP, Bharya S, Al-Sanna'a N, Adatia I, Chitayat D, et al. Abnormal pericyte recruitment as a cause for pulmonary hypertension in Adams-Oliver syndrome. *Am J Med Genet A*. 2004;129A:294-299.

26. Algaze C, Esplin ED, Lowenthal A, Hudgins L, Tacy TA, Selamet Tierney ES. Expanding the phenotype of cardiovascular malformations in Adams-Oliver syndrome. *Am J Med Genet A*. 2013;161A:1386-1389.

27. High FA, Epstein JA. The multifaceted role of Notch in cardiac development and disease. *Nat Rev Genet*. 2008;9:49-61.

28. Oda T, Elkahloun AG, Pike BL, Okajima K, Krantz ID, Genin A, et al. Mutations in the human Jagged1 gene are responsible for Alagille syndrome. *Nat Genet*. 1997;16:235-242.

29. High FA, Lu MM, Pear WS, Loomes KM, Kaestner KH, Epstein JA. Endothelial expression of the Notch ligand Jagged1 is required for vascular smooth muscle development. *Proc Natl Acad Sci U S A*. 2008;105:1955-1959.

30. McDaniell R, Warthen DM, Sanchez-Lara PA, Pai A, Krantz ID, Piccoli DA, Spinner NB. NOTCH2 mutations cause Alagille syndrome, a heterogeneous disorder of the notch signaling pathway. *Am J Hum Genet*. 2006;79:169-173.

31. Isidor B, Lindenbaum P, Pichon O, Bezieau S, Dina C, Jacquemont S, et al. Truncating mutations in the last exon of NOTCH2 cause a rare skeletal disorder with osteoporosis. *Nat Genet*. 2011;43:306-308.

32. Simpson MA, Irving MD, Asilmaz E, Gray MJ, Dafou D, Elmslie FV, et al. Mutations in NOTCH2 cause Hajdu-Cheney syndrome, a disorder of severe and progressive bone loss. *Nat Genet*. 2011;43:303-305.

33. Jiang R, Lan Y, Chapman HD, Shawber C, Norton CR, Serreze DV, et al. Defects in limb, craniofacial, and thymic development in Jagged2 mutant mice. *Genes Dev*. 1998;12:1046-1057.

34. Francis JC, Radtke F, Logan MP. Notch1 signals through Jagged2 to regulate apoptosis in the apical ectodermal ridge of the developing limb bud. *Dev Dyn*. 2005;234:1006-1015.

35. Pan Y, Liu Z, Shen J, Kopan R. Notch1 and 2 cooperate in limb ectoderm to receive an early Jagged2 signal regulating interdigital apoptosis. *Dev Biol*. 2005;286:472-482.

36. Ramasamy SK, Kusumbe AP, Wang L, Adams RH. Endothelial Notch activity promotes angiogenesis and osteogenesis in bone. *Nature*. 2014;507:376-380.

37. Gridley T. Notch signaling in vascular development and physiology. *Development*. 2007;134:2709-2718.

38. Hambleton S, Valeyev NV, Muranyi A, Knott V, Werner JM, McMichael AJ, et al. Structural and functional properties of the human notch-1 ligand binding region. *Structure*. 2004;12:2173-2183.

39. de Celis JF, Barrio R, del Arco A, Garcia-Bellido A. Genetic and molecular characterization of a Notch mutation in its Delta- and Serrate-binding domain in Drosophila. *Proc Natl Acad Sci U S A*. 1993;90:4037-4041.

40. Lu L, Stanley P. Roles of O-fucose glycans in notch signaling revealed by mutant mice. *Methods Enzymol*. 2006;417:127-136.

41. Alfaro JF, Gong CX, Monroe ME, Aldrich JT, Clauss TR, Purvine SO, et al. Tandem mass spectrometry identifies many mouse brain O-GlcNAcylated proteins including EGF domain-specific O-GlcNAc transferase targets. *Proc Natl Acad Sci U S A*. 2012;109:7280-7285.

42. Sakaidani Y, Ichiyanagi N, Saito C, Nomura T, Ito M, Nishio Y, et al. O-linked-N-acetylglucosamine modification of mammalian Notch receptors by an atypical O-GlcNAc transferase Eogt1. *Biochem Biophys Res Commun*. 2012;419:14-19.

43. Cartegni L, Chew SL, Krainer AR. Listening to silence and understanding nonsense: exonic mutations that affect splicing. *Nat Rev Genet*. 2002;3:285-298.

44. Fischer A, Schumacher N, Maier M, Sendtner M, Gessler M. The Notch target genes Hey1 and Hey2 are required for embryonic vascular development. *Genes Dev*. 2004;18:901-911.

TABLE 1: Clinical characteristics of AOS affected subjects harboring *NOTCH1* mutations

Subject ID	Country of origin	Current age	Gender	Scalp ACC	TTLD	Cardiac and/or vascular features [age at diagnosis]	Echocardiographic assessment [age at assessment]	Other features [age at diagnosis]
1-II:1*	UK	29 yr	male	++	+	nd	not assessed	undefined heart murmur
1-II:2		28 yr	male	++	+	nd	not assessed	undefined heart murmur
1-II:4		35 yr	female	–	++	[34 yr]: AR; AS; CMTC on abdomen and legs	[34 yr]: mild AS and AR (PV: 2.04 m/s, PG: 16.65 mmHg), mildly increased velocities through pulmonary valve (2.06 m/s) and descending aorta (2 m/s)	–
1-III:1		17 yr	male	+	++	nd	not assessed	–
1-III:2		10 yr	female	–	–	[9 yr]: AR	[9 yr]: mild AR (PV: 2.21 m/s, PG: 19.54 mmHg), mildly increased velocities through pulmonary valve (1.91 m/s) and descending aorta (2.3 m/s)	–
2-II:1*	Italy	27 yr	male	+	–	[15 d]: BAV; CoA; PMV; [5 mo]: subclavian flap	[15 d]: non-stenotic PMV with mild regurgitation	Ref: Dallapiccola *et al*. 1992 (Patient 2).[15]

						coarctectomy		
3-II:3	Germany	35 yr	male	–	+	–	[34 yr]: normal	–
3-III:1*		8 yr	male	++	+	–	[7 yr]: normal	–
4-I:2	Italy	47 yr	female	–	–	AR; AS	[47 yr]: thick fibrotic semilunar valves; moderate AR (PG: 34 mmHg, MG: 20 mmHg); mild to moderate LVH	long palpebral fissures
4-II:1*		25 yr	female	+	++	[15 d]: AS; CoA; PMV; VSD	[15 d]: subaortic membranous VSD; severe AS (PG: 80 mmHg, MG: 60 mmHg); PMV with valvular insufficiency	long palpebral fissures
5-II:1*	UK	10 yr	male	++	–	[1 d]: PA-VSD; [6 d]: right MBTS; [2 yr]: Rastelli correction	[1 d]: PA, VSD Fallot type; [10 yr]: some narrowing of shunt, free pulmonary regurgitation	[5 yr]: portal vein thrombosis; portal hypertension; T cell lymphopenia; complex learning disability; autism
6-II:1*	Russia	deceased	female	++	+	[*in utero*]: truncus arteriosus communis type I; [1 d]: VSD	[1 d]: membrane VSD, right-sided aortic bow descending on left-hand side	–

7-II:1*	Italy	8 yr	male	+	+	–	[7 yr]: normal	bilateral cryptorchidism; bilateral abdominal wall hernia; hypertelorism; downslanting palpebral fissures
8-II:1*	Italy	15 yr	male	+	+	[1 d]: CMTC	[15 yr]: normal	epilepsy; dyslexia
9-II:1*	Germany	33 yr	female	+	++	nd	not assessed	–
10-II:1*	France	16 yr	female	++	++	[3.5 yr]: ASD; surgically closed at 4 yr; arteriography: EHPVT, hepatopetal and hepatofugal collateral veins	[3.5 yr]: ASD, suspected portopulmonary hypertension (mPAP: 30 mmHg); [7 yr]: mPAP: 45 mmHg, PVR: 8.1 Wood U/m^2, PWP: <15 mmHg; [12 yr]: mPAP: 27 mmHg with Sildenafil treatment	[3.5 yr]: HSM and portal hypertension with GI bleeding; OPV. Ref: Girard *et al*. 2005 (Patient 1);[16] Franchi-Abella *et al*. 2014.[17]
11-II:1*	Greece	19 yr	male	++	++	[6.5 yr]: arteriography: EPVO, large hepatofugal coronary vein, tiny hepatopetal cavernoma	[6.5 yr]: normal; [14 yr]: normal	[6.5 yr]: HSM and portal hypertension; OPV. Ref: Girard *et al*. 2005 (Patient 2);[16] Franchi-Abella *et al*. 2014.[17]

Key: –, absent; +, present (for ACC: +, small defect (<5 cm); ++, large defect (>5 cm) with underlying osseous skull defect; for TTLD: +, feet or hands only; ++, both feet and hands affected); ACC, aplasia cutis congenita; AR, aortic regurgitation; AS, aortic valve stenosis; ASD, atrial septal defect; BAV, bicuspid aortic valve; CMTC, cutis marmorata telangiectatica congenita; CoA, coarctation of the aorta; EPVO, extra-hepatic portal vein obstruction; EHPVT, extra-hepatic portal vein thrombosis; GI, gastrointestinal; HSM, hepatosplenomegaly; LVH, left ventricular hypertrophy; MBTS, modified Blalock–Taussig shunt; MG: median gradient; mPAP, mean pulmonary arterial pressure (measured by right heart catheterization); nd, not determined; OPV, obliterative portal venopathy; PA, pulmonary atresia; PG, peak gradient; PMV, parachute mitral valve; PV, peak velocity; PVR, pulmonary vascular resistance; PWP, pulmonary wedge pressure; Ref:, reference of case report; TTLD, terminal transverse limb defects; VSD, ventral septal defect. Subject identifiers refer to the pedigree structures in Figure 1. The proband for each family is marked with an asterisk.

FIGURE LEGENDS:

Figure 1. Clinical features of three representative AOS patients with *NOTCH1* mutation. (left) Patient 3-III:1 at age 2.8 years: residual skin defect after multiple operations on a large area of scalp aplasia cutis congenita; minor hypoplasia of terminal phalanges of the toes; normal fingers. (middle) Patient 6-II:1 as a newborn: large scalp defect involving the underlying bone; hypoplasia of terminal phalanges of both feet. (right) Patient 8-II:1 at age 14.7 years: small area of alopecia marking a healed scalp defect; hypoplasia of terminal phalanges and nails of the left foot; normal fingers.

Figure 2. Pedigree structures and sequence chromatograms of identified *NOTCH1* mutations. Asterisks denote the families included in the exome sequencing discovery cohort. Probands are marked by the black arrows and asymptomatic carriers are indicated with black dots. For *de novo* mutations, paternity was confirmed by microsatellite analysis (data not shown). **Key:** +, wild-type allele; –, mutant allele.

Figure 3. Location and conservation of NOTCH1 mutations. (A) Schematic of the NOTCH1 protein highlighting the critical functional domains. The AOS mutations identified in this study are arrayed below the schematic. Truncating mutations are marked in green type and orange depicts missense mutations. (B) Conservation of the 6 missense mutations across species. Conserved residues are highlighted in orange. The 4^{th}, 5^{th} and 6^{th} conserved cysteines within the EGF domains are boxed. Accession numbers: *H. sapiens*: NP_060087.3; *M. mulatta*: AFH32544.1; *C. lupus familiaris*: XP_005625490.1 (predicted); *M. musculus*: NP_032740.3; *G. gallus*: NP_001025466.1; *X. tropicalis*: NP_001090757.1; *D. rerio*: NP_571377.2; *T. rubripes*: XP_003975158.1 (predicted); *D. melanogaster*: NP_476859.2.

Figure 4. Ball and stick representation of the 3-dimensional structure of human NOTCH1 EGF repeats 11-13. The positions of the adjacent AOS mutations p.R448Q and p.C449R are highlighted by the solid red arrows. The p.C456Y mutation is similarly marked. The solid black arrows indicate

the disulfide bonds which would be abolished by the p.C449R and p.C456Y mutations, respectively. The side chains of the key Ca^{2+} ion coordinating residues (Asp452, Glu455 and Asp469) and Glu424 are indicated. Water molecules have been removed for clarity. Figure produced from the crystal structure (PDB ID: 2VJ3)[22] using the PyMOL Molecular Graphics System.

Figure 5. Real-time PCR of *NOTCH1*-positive patient samples. Graphs show levels of gene expression for (A) *NOTCH1*, (B) *HEY1* and (C) *HES1*. Relative quantification of mRNA transcripts are calculated relative to the WT baseline value (set at 1) and normalized to endogenous *GAPDH* and *ACTB* levels. Graphs represent the mean of three independent experiments with error bars indicating SEM. The brackets denote individuals with identical *NOTCH1* mutations. **Key:** **p*<0.001; †*p*<0.01

Figure 6. Simplified schematic of the canonical Notch signaling pathway. (A) The EGF-repeat domain of Notch is known to be glycosylated by EOGT in mammalian cells. Activation of the Notch signaling cascade is initiated by the binding of one of five ligands through direct contact of adjacent cells. (B) Ligand activation leads to cleavage and release of NICD, which translocates to the nucleus to form an active transcriptional complex with RBPJ, mastermind (MAML) and transcriptional co-activators (CoA). (C) In the absence of Notch activation, RBPJ complexes with co-repressor proteins (CoR) to repress transcription of downstream genes. Mutations in EOGT and RBPJ have previously been identified in AOS.

FIGURE 1:

FIGURE 2:

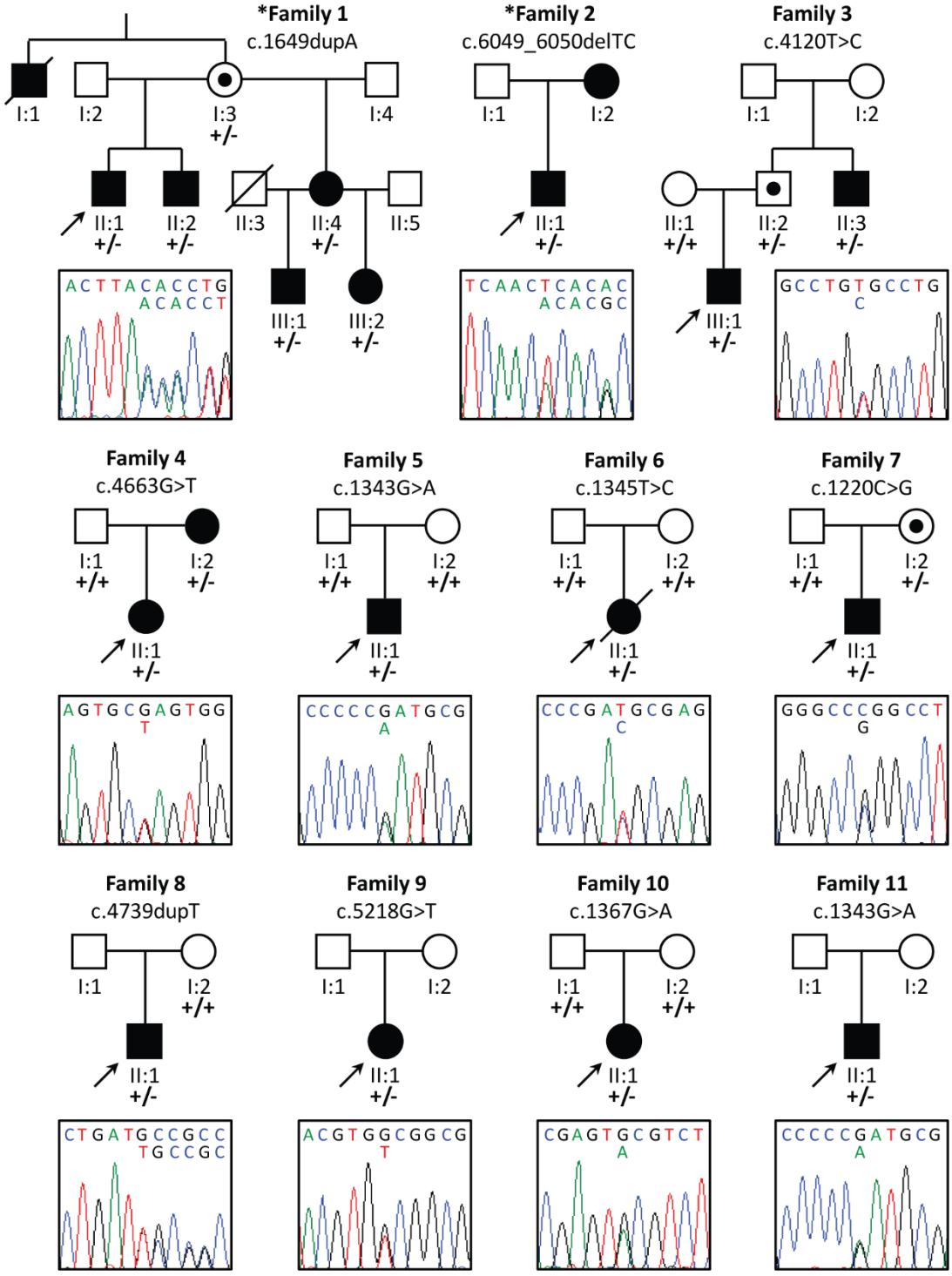
*Family 1
c.1649dupA
I:1
I:2
I:3
+/-
I:4
II:1
+/-
II:2
+/-
II:3
II:4
+/-
II:5
III:1
+/-
III:2
+/-
*Family 2
c.6049_6050delTC
I:1
I:2
II:1
+/-
Family 3
c.4120T>C
I:1
I:2
II:1
+/+
II:2
+/-
II:3
+/-
III:1
+/-
Family 4
c.4663G>T
I:1
+/+
I:2
+/-
II:1
+/-
Family 5
c.1343G>A
I:1
+/+
I:2
+/+
II:1
+/-
Family 6
c.1345T>C
I:1
+/+
I:2
+/+
II:1
+/-
Family 7
c.1220C>G
I:1
+/+
I:2
+/-
II:1
+/-
Family 8
c.4739dupT
I:1
I:2
+/+
II:1
+/-
Family 9
c.5218G>T
I:1
I:2
II:1
+/-
Family 10
c.1367G>A
I:1
+/+
I:2
+/+
II:1
+/-
Family 11
c.1343G>A
I:1
I:2
II:1
+/-

FIGURE 3:

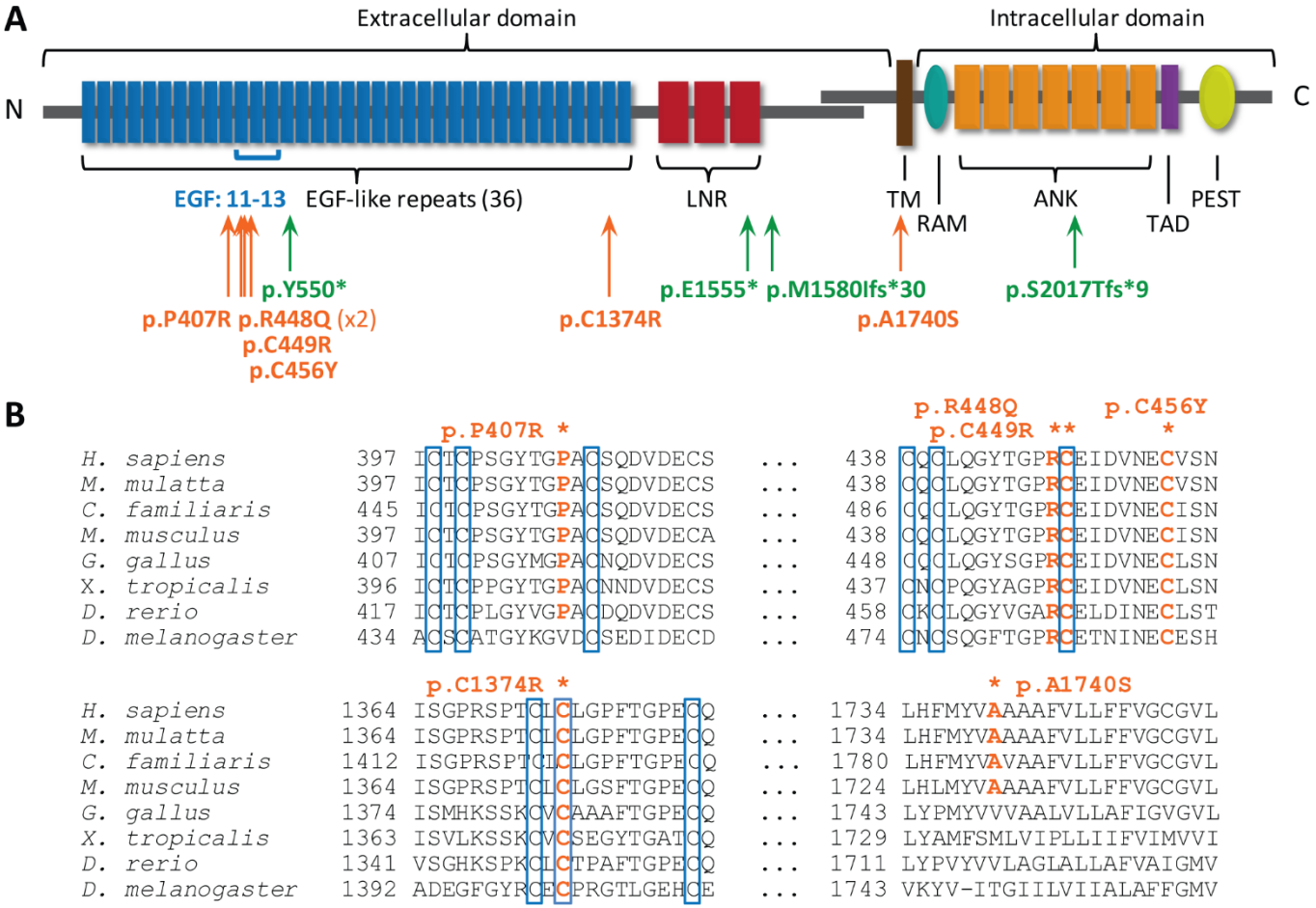
A
Extracellular domain
Intracellular domain
N
C
EGF: 11-13
EGF-like repeats (36)
LNR
TM
RAM
ANK
TAD
PEST
p.Y550*
p.P407R
p.R448Q (x2)
p.C449R
p.C456Y
p.C1374R
p.E1555*
p.M1580Ifs*30
p.A1740S
p.S2017Tfs*9
B
p.P407R *
p.R448Q
p.C449R **
p.C456Y
*
H. sapiens 397 ICTCPSGYTGPACSQDVDECS ... 438 CQCLQGYTGPRCEIDVNECVSN
M. mulatta 397 ICTCPSGYTGPACSQDVDECS ... 438 CQCLQGYTGPRCEIDVNECVSN
C. familiaris 445 ICTCPSGYTGPACSQDVDECS ... 486 CQCLQGYTGPRCEIDVNECISN
M. musculus 397 ICTCPSGYTGPACSQDVDECA ... 438 CQCLQGYTGPRCEIDVNECISN
G. gallus 407 ICTCPSGYMGPACNQDVDECS ... 448 CQCLQGYSGPRCEIDVNECLSN
X. tropicalis 396 ICTCPPGYTGPACNNDVDECS ... 437 CNCPQGYAGPRCEIDVNECLSN
D. rerio 417 ICTCPLGYVGPACDQDVDECS ... 458 CKCLQGYVGARCELDINECLST
D. melanogaster 434 ACSCATGYKGVDCSEDIDECD ... 474 CNCSQGFTGPRCETNINECESH
p.C1374R *
* p.A1740S
H. sapiens 1364 ISGPRSPTCLCLGPFTGPECQ ... 1734 LHFMYVAAAAFVLLFFVGCGVL
M. mulatta 1364 ISGPRSPTCLCLGPFTGPECQ ... 1734 LHFMYVAAAAFVLLFFVGCGVL
C. familiaris 1412 ISGPRSPTCLCLGPFTGPECQ ... 1780 LHFMYVAVAAFVLLFFVGCGVL
M. musculus 1364 ISGPRSPTCLCLGSFTGPECQ ... 1724 LHLMYVAAAAFVLLFFVGCGVL
G. gallus 1374 ISMHKSSKCVCAAAFTGPECQ ... 1743 LYPMYVVVAALVLLAFIGVGVL
X. tropicalis 1363 ISVLKSSKCVCSEGYTGATCQ ... 1729 LYAMFSMLVIPLLIIFVIMVVI
D. rerio 1341 VSGHKSPKCLCTPAFTGPECQ ... 1711 LYPVYVVLAGLALLAFVAIGMV
D. melanogaster 1392 ADEGFGYRCECPRGTLGEHCE ... 1743 VKYV-ITGIILVIIALAFFGMV

FIGURE 4:

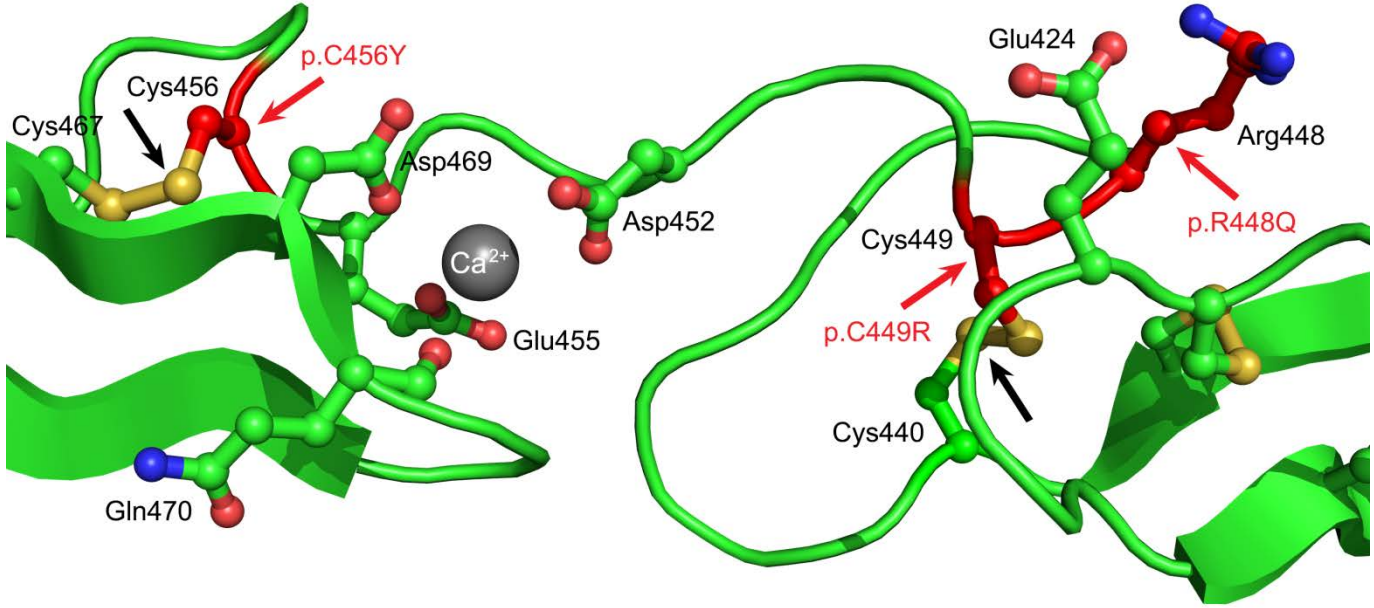
p.C456Y
Cys456
Cys467
Asp469
Asp452
Ca2+
Glu455
Gln470
Glu424
Arg448
p.R448Q
Cys449
p.C449R
Cys440

FIGURE 5:

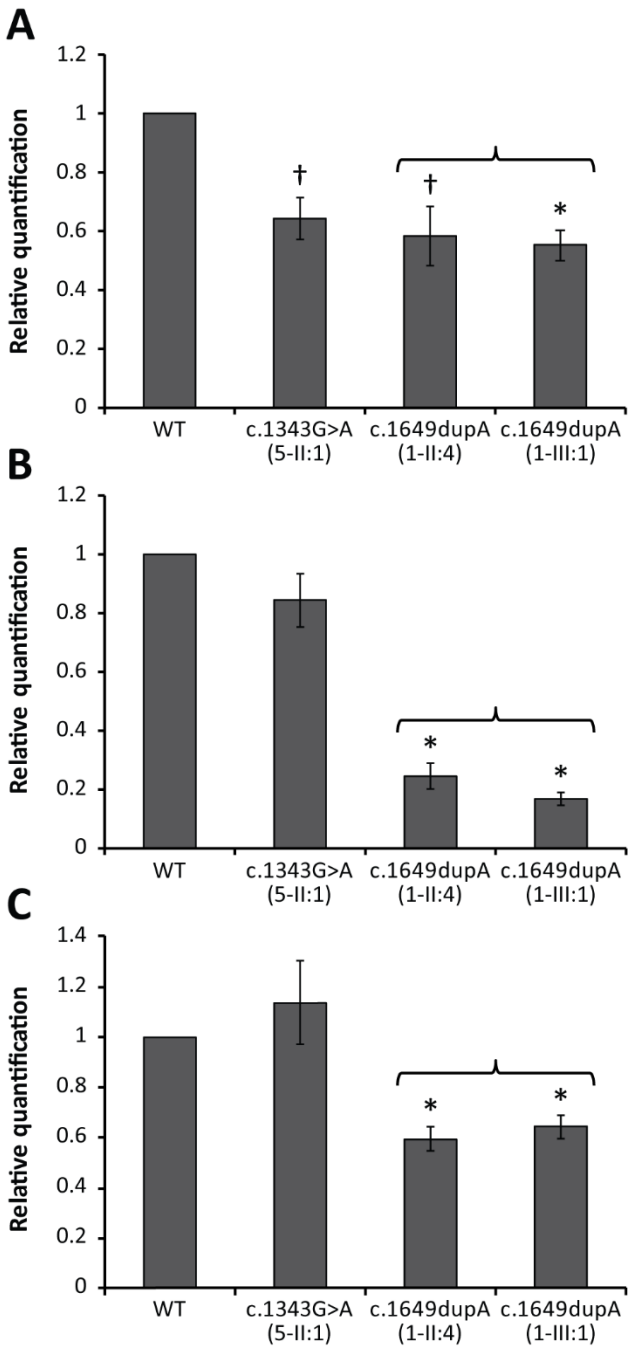
A
Relative quantification
1.2
1
0.8
0.6
0.4
0.2
0
†
†
*
WT
c.1343G>A (5-II:1)
c.1649dupA (1-II:4)
c.1649dupA (1-III:1)
B
Relative quantification
1.2
1
0.8
0.6
0.4
0.2
0
*
*
WT
c.1343G>A (5-II:1)
c.1649dupA (1-II:4)
c.1649dupA (1-III:1)
C
Relative quantification
1.4
1.2
1
0.8
0.6
0.4
0.2
0
*
*
WT
c.1343G>A (5-II:1)
c.1649dupA (1-II:4)
c.1649dupA (1-III:1)

FIGURE 6:

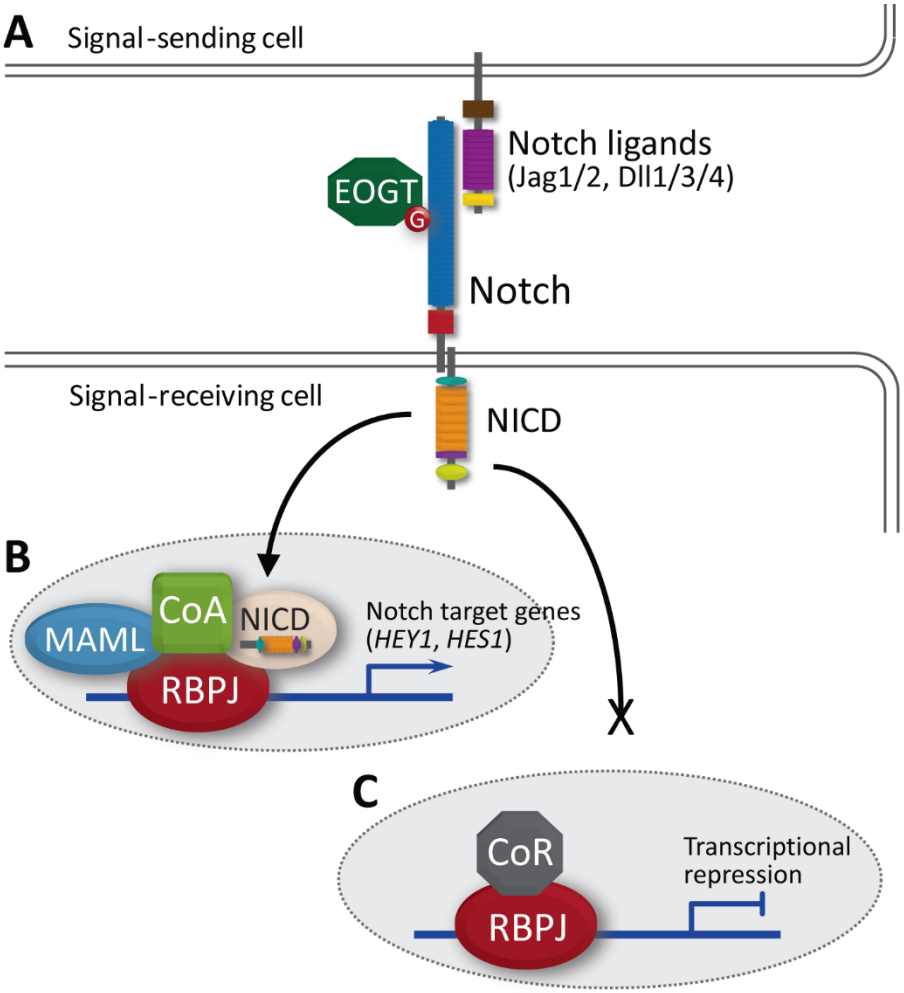
A
Signal-sending cell
Notch ligands
(Jag1/2, Dll1/3/4)
EOGT
G
Notch
Signal-receiving cell
NICD
B
MAML
CoA
NICD
RBPJ
Notch target genes
(HEY1, HES1)
C
CoR
RBPJ
Transcriptional
repression

SUPPLEMENTAL MATERIAL

SUPPLEMENTAL TABLE I. Summary of identified *NOTCH1* variants

Exon	Coding variant	Protein variant	Variant type	Protein domain
7	c.1220C>G	p.P407R	Missense	EGF 10
8	c.1343G>A	p.R448Q	Missense	EGF 11
8	c.1345T>C	p.C449R	Missense	EGF 11
8	c.1367G>A	p.C456Y	Missense	EGF 11
10	c.1649dupA	p.Y550*	Frameshift	EGF 14
25	c.4120T>C	p.C1374R	Missense	EGF 35
26	c.4663G>T	p.E1555*	Nonsense	LNR 3
26	c.4739dupT	p.M1580Ifs*30	Frameshift	-
28	c.5218G>T	p.A1740S	Missense	TM
32	c.6049_6050delTC	p.S2017Tfs*9	Frameshift	ANK 4

Key to abbreviations: EGF, epidermal growth factor-like repeat domain; LNR, Lin-12 NOTCH repeat domain; TM, transmembrane domain; ANK, ankyrin repeat domain.

SUPPLEMENTAL TABLE II. Predicted pathogenicity of identified *NOTCH1* variants

Variant	MutationTaster2	PolyPhen-2	SIFT Protein
p.P407R	Disease causing (prob: 0.999)	Probably damaging (0.968)	Tolerated (0.51)
p.R448Q	Disease causing (prob: 0.999)	Probably damaging (0.984)	Tolerated (0.29)
p.C449R	Disease causing (prob: 0.999)	Probably damaging (1.000)	Damaging (0)
p.C456Y	Disease causing (prob: 0.999)	Probably damaging (1.000)	Damaging (0)
p.Y550*	Disease causing (prob: 1)	n/a	n/a
p.C1374R	Disease causing (prob: 0.999)	Probably damaging (0.999)	Damaging (0)
p.E1555*	Disease causing (prob: 1)	n/a	n/a
p.M1580Ifs*30	Disease causing (prob: 1)	n/a	n/a
p.A1740S	Polymorphism (prob: 0.980)	Benign (0.134)	Tolerated (0.42)
p.S2017Tfs*9	Disease causing (prob: 1)	n/a	n/a

SUPPLEMENTAL FIGURE I. Real-time PCR of transient transfections

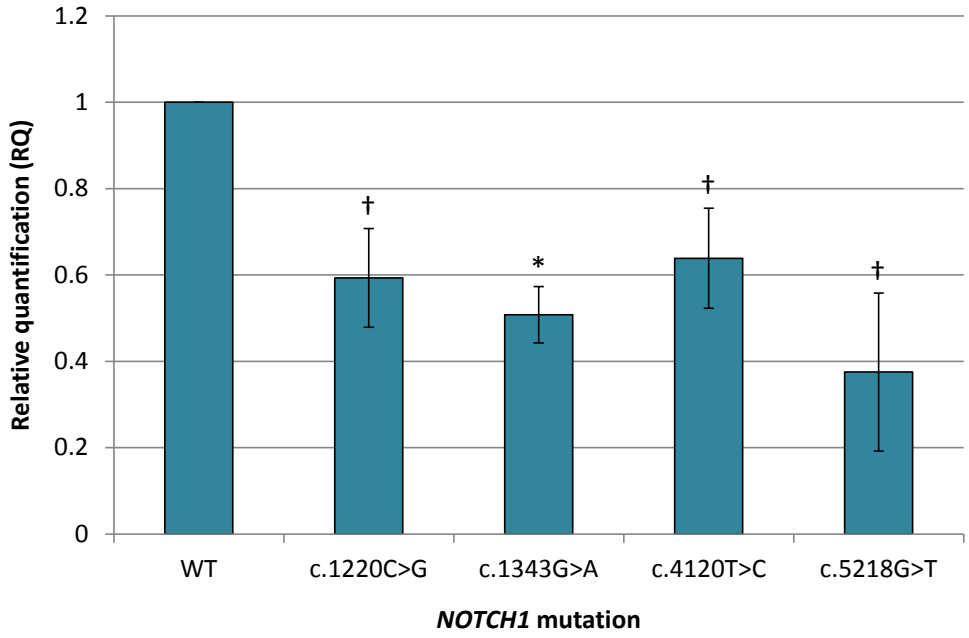

Real-time quantitative PCR of cells transiently transfected with mutagenized *NOTCH1* cDNA constructs. All missense mutations tested demonstrate reduced *NOTCH1* transcript level by comparison to cells transfected with a full-length wild-type construct (WT). Relative quantification of gene expression is calculated relative to the WT baseline value (set to 1) and normalized to *GAPDH* and *ACTB*. Graphs represent the mean of three independent experiments with error bars indicating SEM. **Key:** **p*<0.01; †*p*<0.05